Electronic Supplementary Material (ESI) for Energy & Environmental Science.

High thermoelectric performance of p-BiSbTe compounds prepared by ultra-fast thermally induced reaction

Gang Zheng,[a] Xianli Su,[a, c, †] Hongyao Xie,[a] Yuejiao Shu,[a] Tao Liang,[a] Xiaoyu She,[a] Wei Liu,[a] Yonggao Yan,[a] Qingjie Zhang, [a] Ctirad Uher,[b] Mercouri G Kanatzidis,[c, †] Xinfeng Tang[a, †]

[a] *State Key Laboratory of Advanced Technology for Materials Synthesis and Processing, Wuhan University of Technology, Wuhan 430070, China*

[b] *Department of Physics, University of Michigan, Ann Arbor, Michigan 48109, USA*

[c] *Department of Chemistry, Northwestern University, Evanston, Illinois 60208, USA*

[†] Correspondence to: X. Su (suxianli@whut.edu.cn), M. G. K. (m-kanatzidis@northwestern.edu), X. Tang (tangxf@whut.edu.cn).

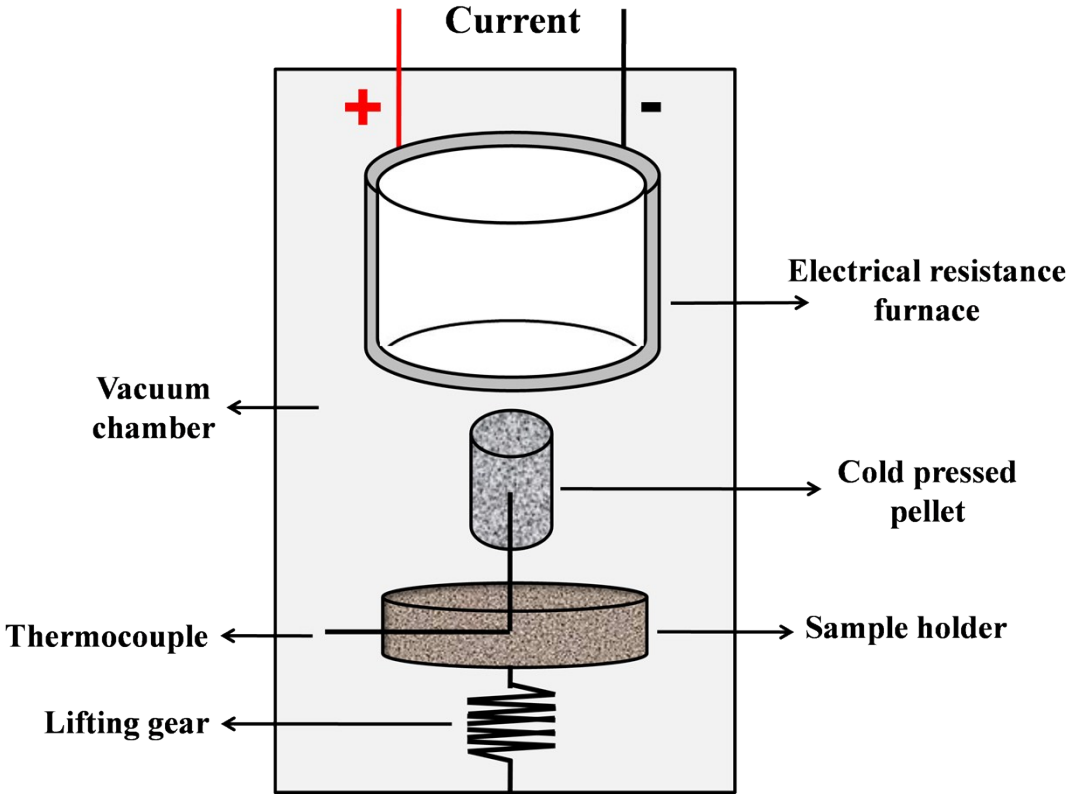

Figure S1: Schematic diagram of an apparatus to measure the temperature profile during the thermally induced flash synthesis

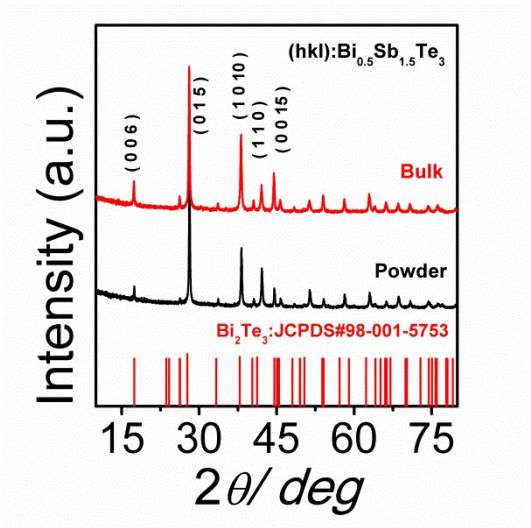

Figure S2: XRD patterns of $Bi_{0.5}Sb_{1.5}Te_3$ after TIFS and PAS processing.

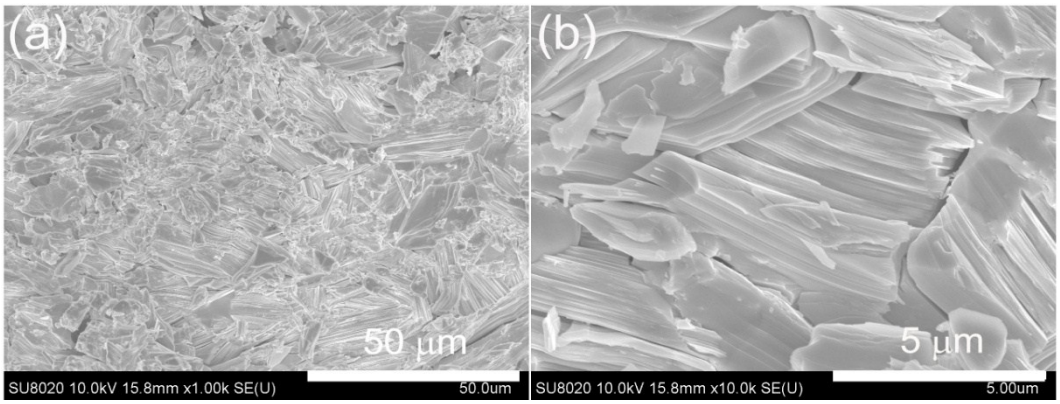

Figure S3: (a) FESEM of $Bi_{0.5}Sb_{1.5}Te_3$ processed by TIFS -PAS; (b) high-magnification FESEM of $Bi_{0.5}Sb_{1.5}Te_3$ processed by TIFS-PAS.

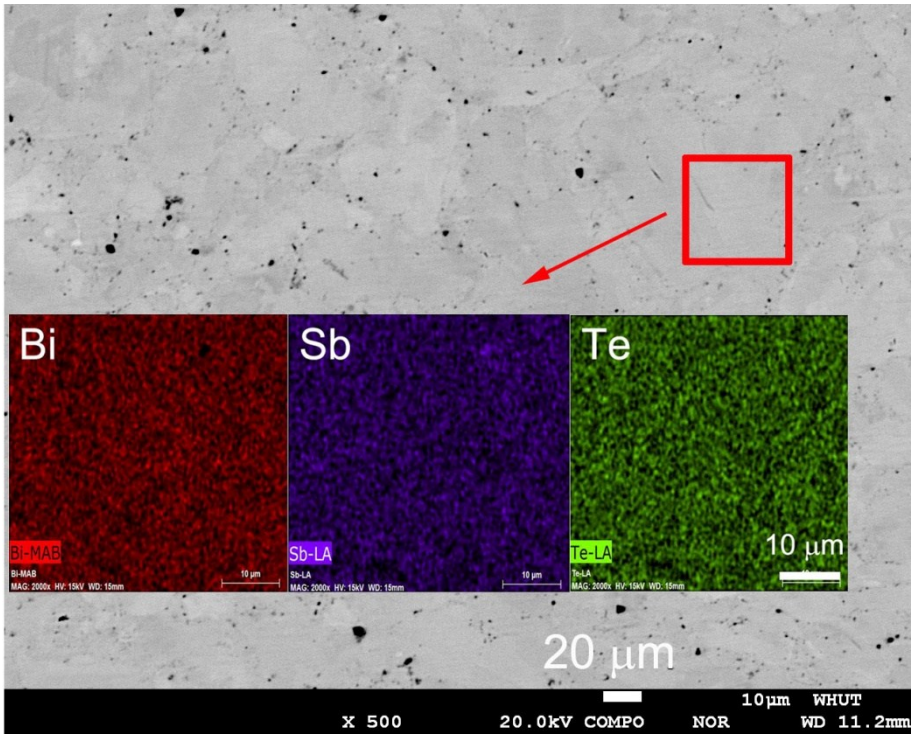

Figure S4: Back-scattered electron image of a polished surface of $Bi_{0.5}Sb_{1.5}Te_3$ processed by thermally induced flash synthesis at 823 K for 3 min. Insets show elemental distributions.

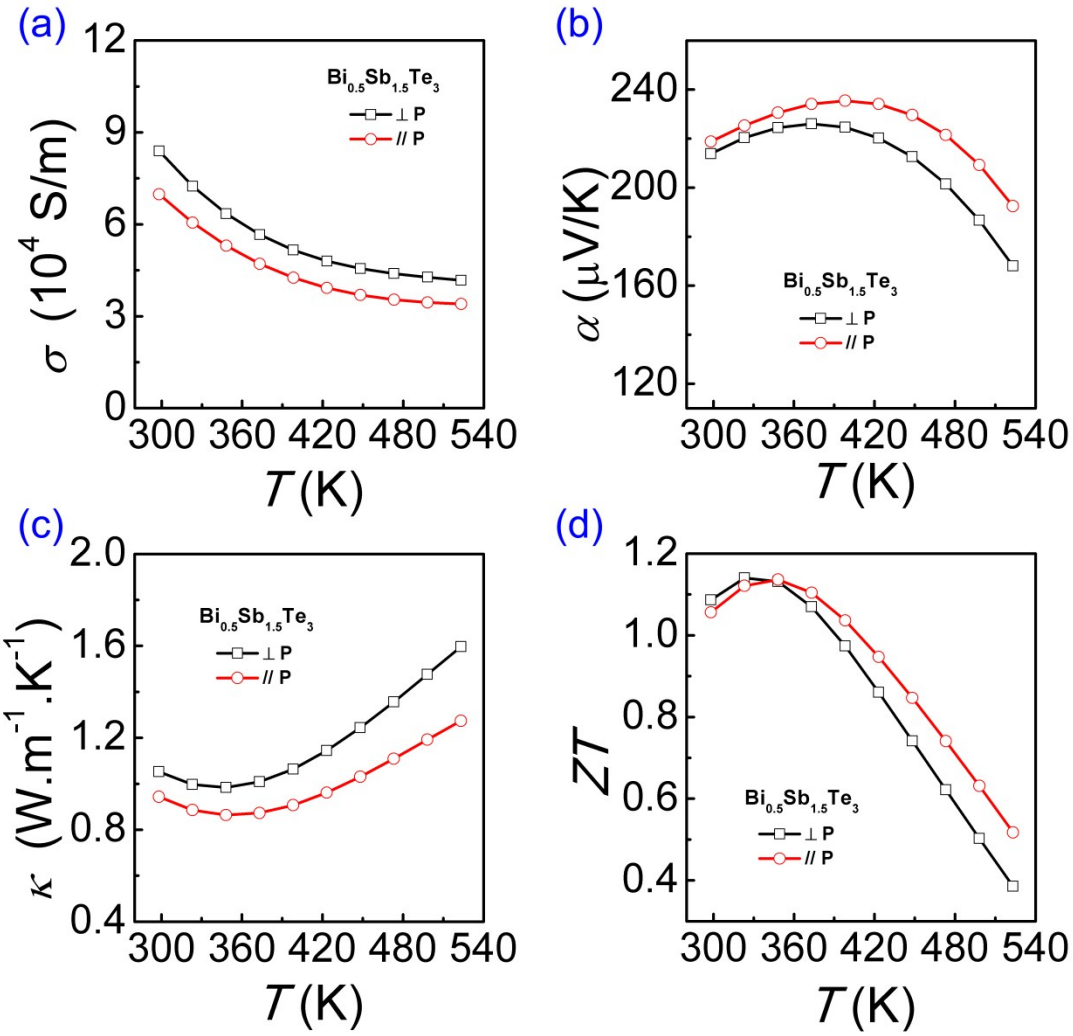

Figure S5: Thermoelectric properties of $Bi_{0.5}Sb_{1.5}Te_3$ processed by TIFS-PAS. (a) Electrical conductivity; (b) Seebeck coefficient; (c) Thermal conductivity; (d) Dimensionless figure of merit *ZT*.

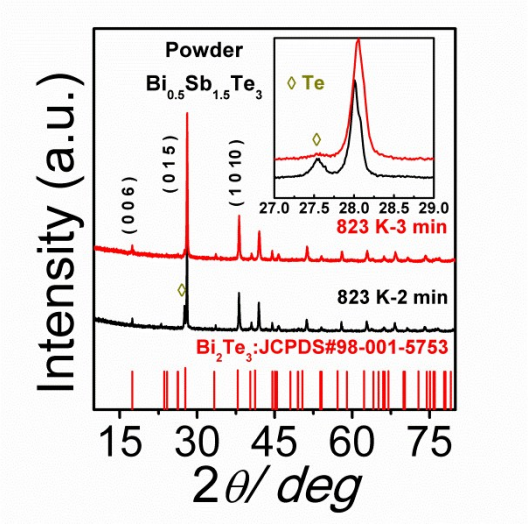

Figure S6: XRD patterns of $Bi_{0.5}Sb_{1.5}Te_3$ after thermally induced flash synthesis at 823 K for 2 min and 3 min duration. The inset is an expanded view of the 2θ interval between 27^0 and 29^0.

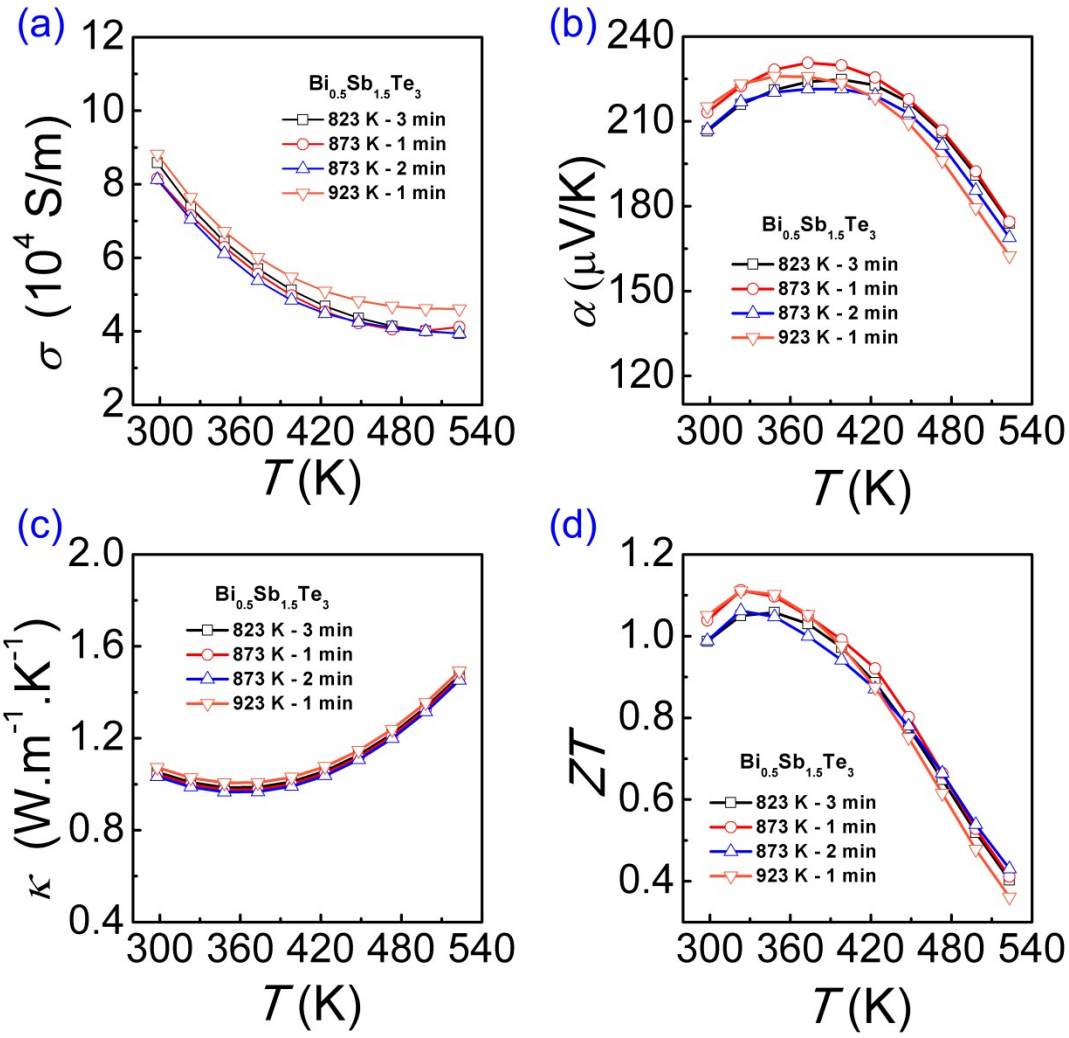

Figure S7: Thermoelectric properties of $Bi_{0.5}Sb_{1.5}Te_3$ processed under different thermally induced flash synthesis parameters.
(a) Electrical conductivity; (b) Seebeck coefficient; (c) Thermal conductivity; (d) Dimensionless figure of merit *ZT*.

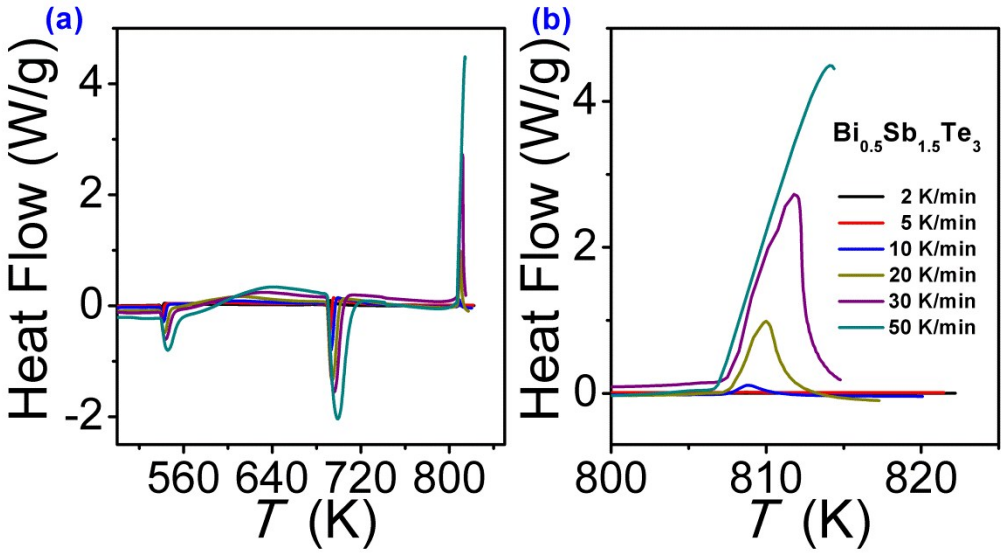

Figure S8: Heat flow curve of $Bi_{0.5}Sb_{1.5}Te_3$ showing signatures of the presence of Bi, Sb and Te at different temperatures (the upper peak and valley are corresponding to exothermic and endothermic process respectively.):
(a) Temperature range of 500 K~850 K; (b) Detailed view of the 800 K ~825 K range.

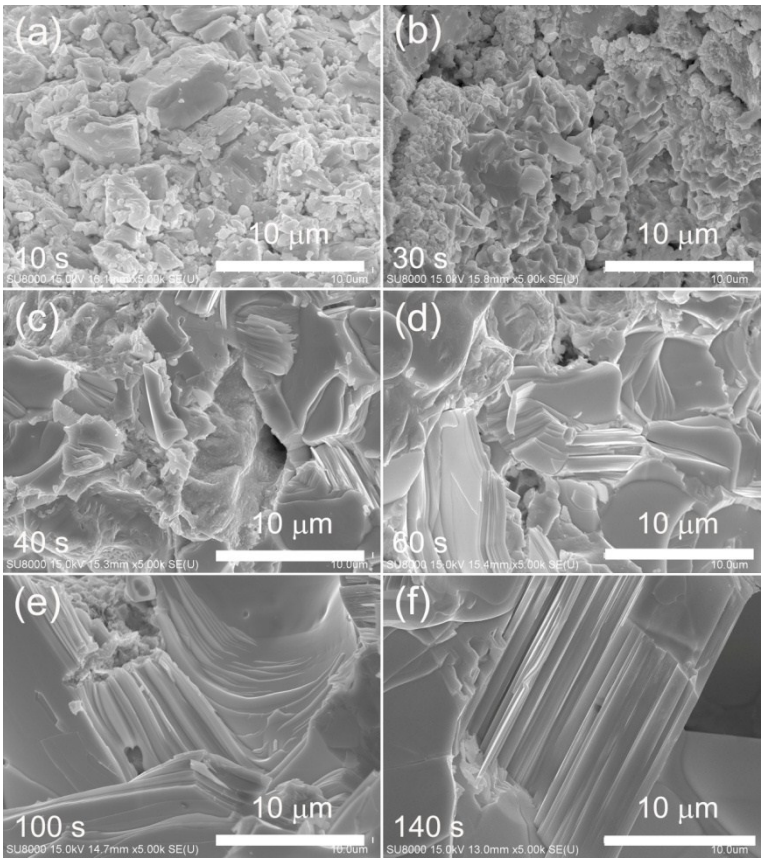

Figure S9: FESEM images of $Bi_{0.5}Sb_{1.5}Te_3$ at different stage of thermally induced flash synthesis process at 823 K (a) 10 s; (b) 30 s; (c) 40 s; (d) 60 s; (e) 100 s; (f) 140 s.

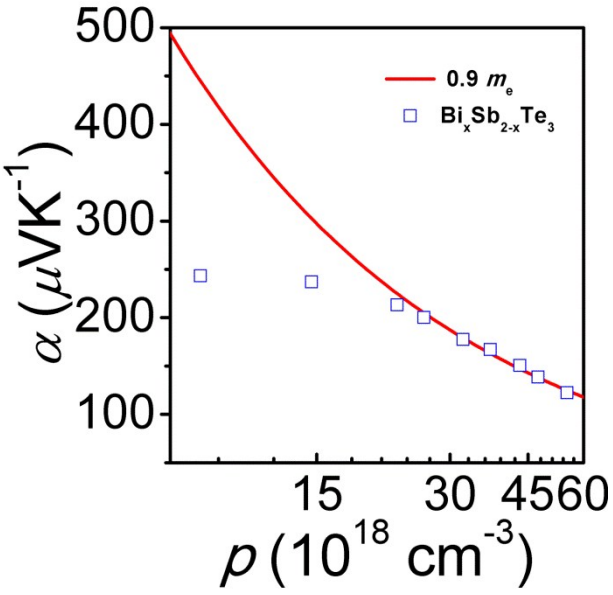

Figure S10: Room temperature Seebeck coefficient of $Bi_xSb_{2-x}Te_3$ samples synthesized by TIFS-PAS and plotted as a function of the carrier concentration (the Pisarenko plot)

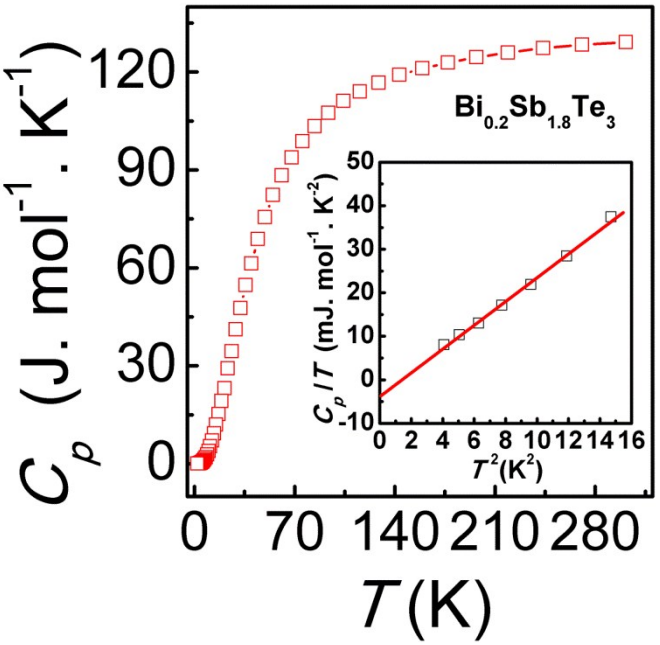

Figure S11: Temperature dependence of the heat capacity of $Bi_{0.2}Sb_{1.8}Te_3$ synthesized by TIFS-PAS.

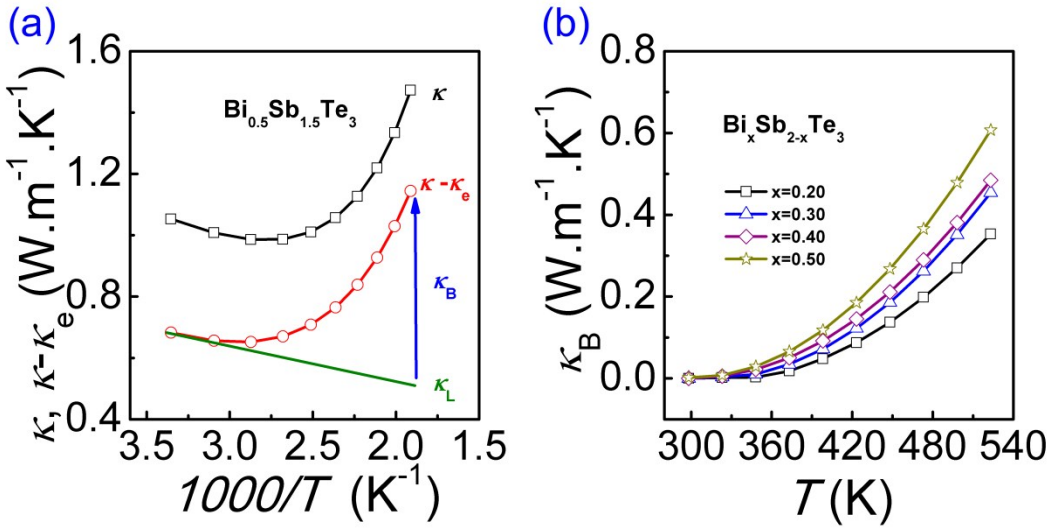

Figure S12: (a) Bipolar thermal conductivity of $Bi_{0.5}Sb_{1.5}Te_3$ synthesized by TIFS-PAS; (b) Temperature dependence of the bipolar thermal conductivity of $Bi_xSb_{2-x}Te_3$ synthesized by TIFS-PAS.

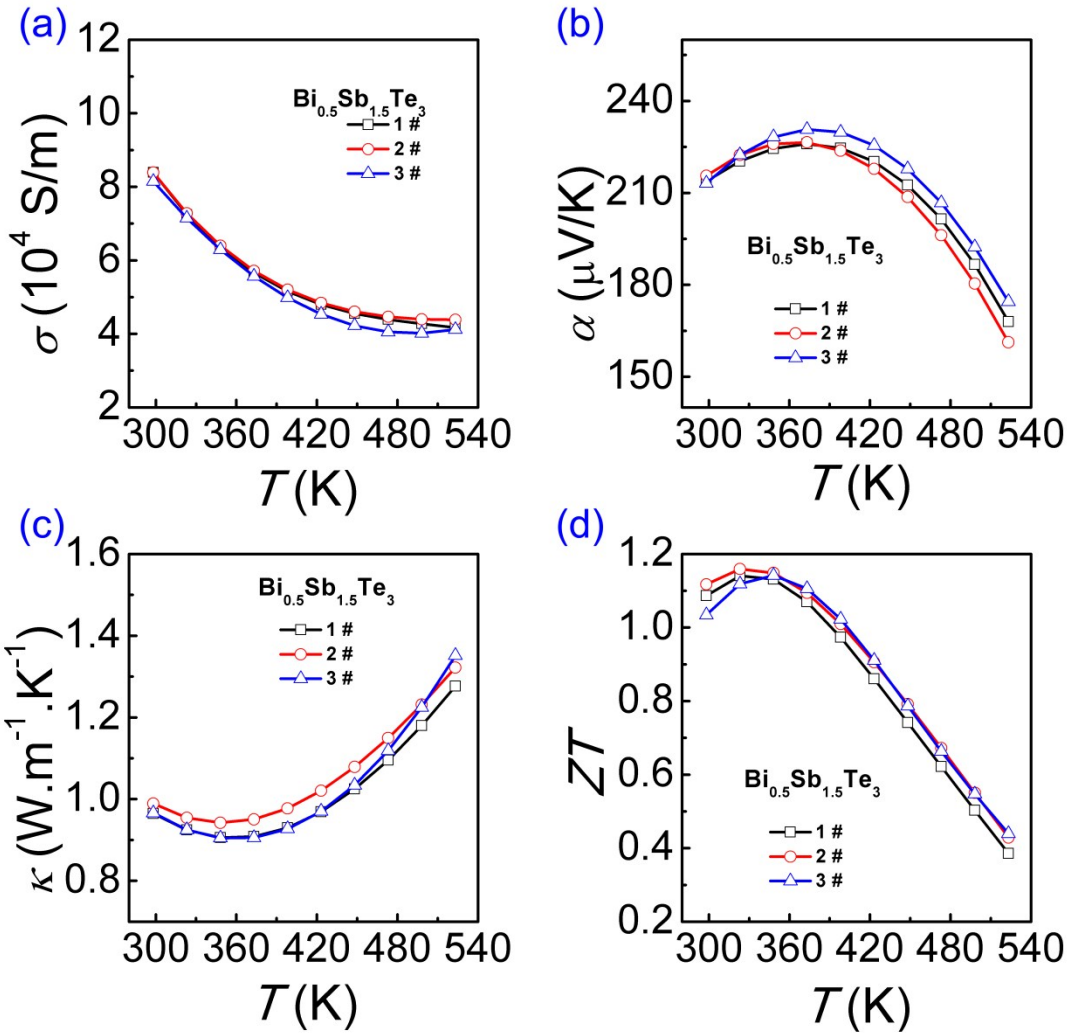

Figure S13: Thermoelectric properties of $Bi_{0.5}Sb_{1.5}Te_3$ samples processed by three independent TIFS-PAS syntheses.
(a) Electrical conductivity; (b) Seebeck coefficient; (c) Thermal conductivity;
(d) Dimensionless figure of merit *ZT*.

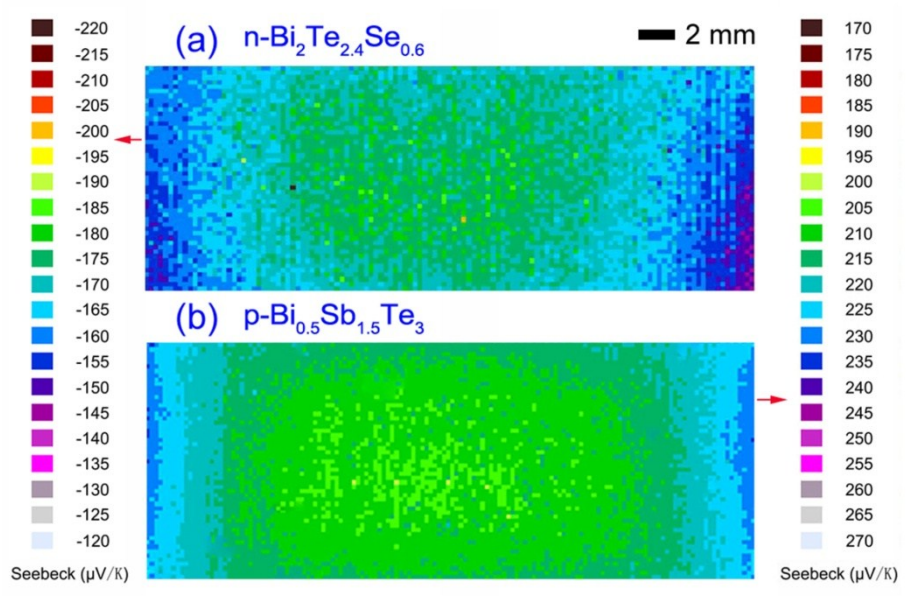

Figure S14: Distribution of Seebeck coefficients over the cross section of samples with the size Φ 30×12 mm^3. (a) n-$Bi_2Te_{2.4}Se_{0.6}$; (b) p-$Bi_{0.5}Sb_{1.5}Te_3$.

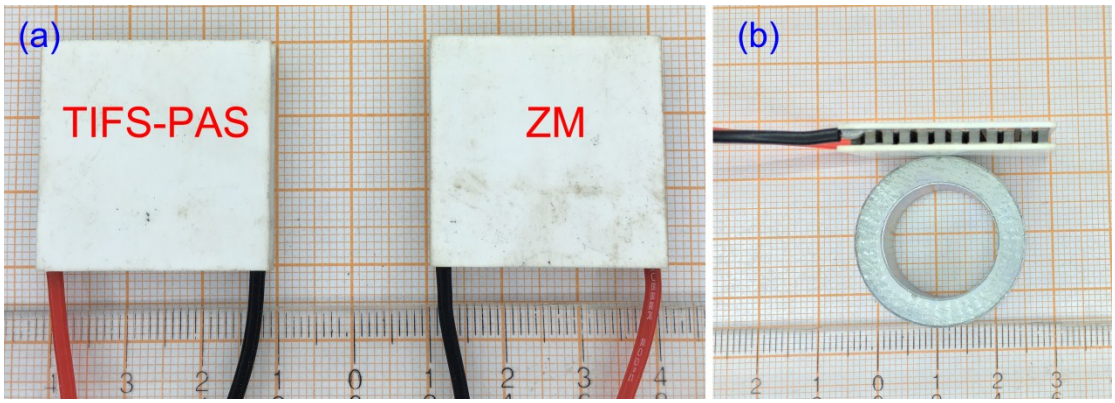

Figure S15: (a) and (b) Image of Modules (30×30×3.8 mm^3) assembled from TIFS-PAS thermoelectric materials and Zone Melting ingots (ZM) with a total of 71 pairs of n-p Bi_2Te_3 based materials for each module.

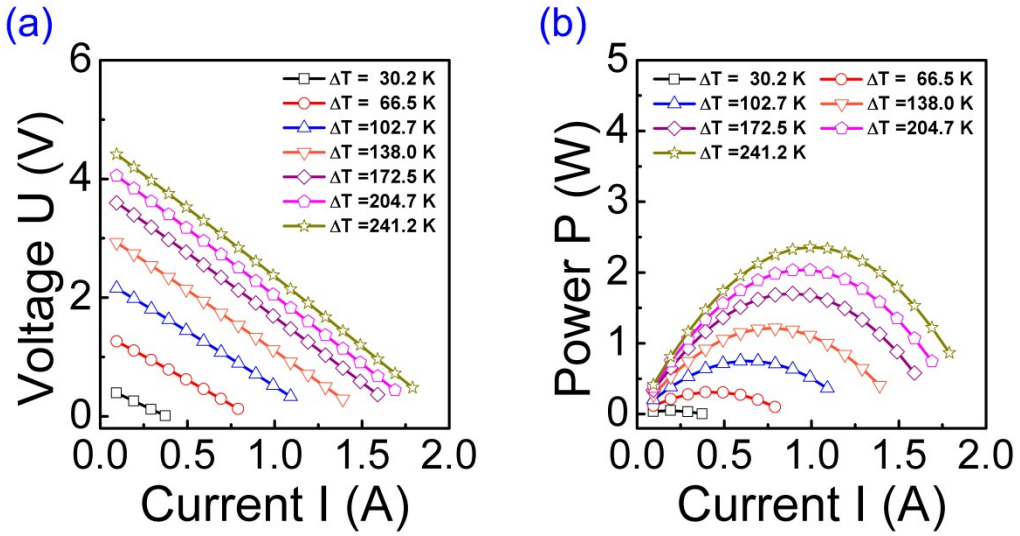

Figure S16: The output performance of a commercial module fabricated by using Zone Melting ingot materials.

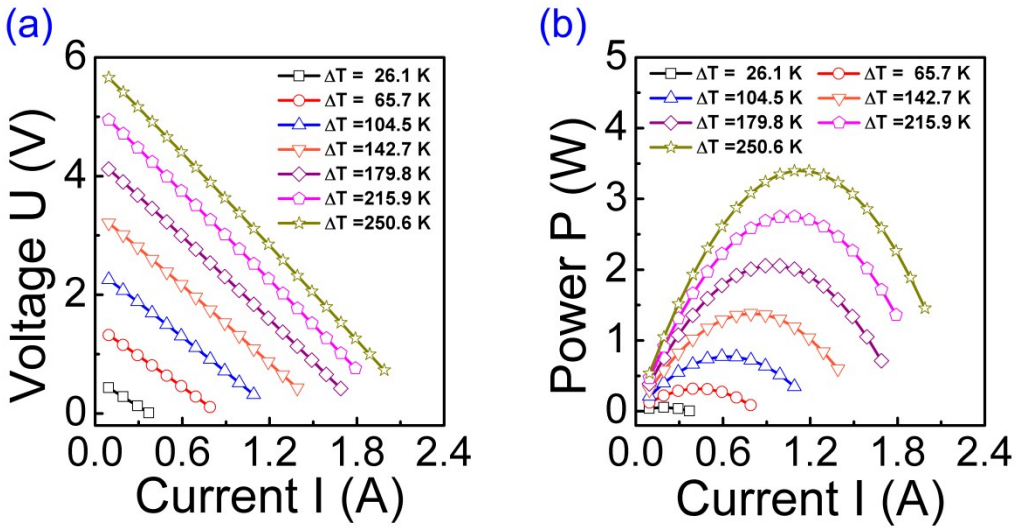

Figure S17: The output performance of a module fabricated from TIFS-PAS-processed materials.

Table S1. Fitting parameters for the heat capacity of $Bi_xSb_{2-x}Te_3$ (x=0.0~0.6) compounds.

	α (mJ mol^{-1} K^{-2})	β (mJ mol^{-1} K^{-2})	A_1 (J mol^{-1} K^{-2})	Θ_{E1} (K)	A_2 (J mol^{-1} K^{-2})	Θ_{E2} (K)	m^*/m_e	θ_D (K)
0.00	0.32	2.09	1.74	33	13.58	63	0.47	167
0.20	0.55	2.23	3.11	38	18.10	74	0.92	163
0.30	0.53	2.33	2.38	36	10.52	64	1.03	161
0.40	0.52	2.39	1.38	31	10.88	56	1.05	160
0.50	0.50	2.45	2.72	36	10.66	64	1.14	158
0.60	0.26	2.60	3.99	39	7.11	62	0.83	155

Table S2. Performance parameters of the fabricated modules.

	T/℃	△T/	T_h/℃	T_c/℃	Q/J s^{-1}	R_2/Ω	R_{1max}/Ω	P_{max}/W	η_{max}/%
100	ZM	66.5	81.9	15.4	14.3	1.63	2.01	0.31	2.17
100	TIFS-PAS	65.7	80.2	14.5	15.7	1.74	2.00	0.32	2.01
150	ZM	102.7	122.2	19.5	24.1	1.83	2.13	0.75	3.11
150	TIFS-PAS	104.5	122.8	18.3	25.0	1.95	2.10	0.78	3.08
200	ZM	138.0	162.2	24.2	32.5	2.04	2.51	1.21	3.70
200	TIFS-PAS	142.7	165.0	22.3	34.7	2.15	2.28	1.38	3.97
250	ZM	172.5	201.0	28.5	42.9	2.16	2.14	1.70	3.92
250	TIFS-PAS	179.8	205.9	26.1	44.4	2.32	2.52	2.06	4.62
300	ZM	204.7	238.1	33.4	53.1	2.26	2.07	2.03	3.83
300	TIFS-PAS	215.9	246.1	30.2	54.3	2.47	2.57	2.75	5.04
350	ZM	241.2	279.2	38.0	64.5	2.32	2.40	2.35	3.65
350	TIFS-PAS	250.6	285.2	34.6	64.8	2.61	2.61	3.40	5.22